

Surface grafting of carbon fibers with artificial silver-nanoparticle-decorated graphene oxide for high-speed electrical actuation of shape-memory polymers

Haibao Lu,¹ Shipeng Zhu,² Yunhua Yang,² Wei Min Huang,³ Jinsong Leng,¹ Shanyi Du¹

¹Science and Technology of Advanced Composites in Special Environments Laboratory, Harbin Institute of Technology, Harbin 150080, China

²Science and Technology of Advanced Functional Composites Laboratory, Aerospace Research Institute of Materials and Processing Technology, Beijing 100076, China

³School of Mechanical and Aerospace Engineering, Nanyang Technological University, 50 Nanyang Avenue, Singapore 639798
Correspondence to: H. Lu (E-mail: luhb@hit.edu.cn)

ABSTRACT: Poor heat conduction in the interface between the carbon fiber and polymer matrix is a problem in the actuation of shape-memory polymer (SMP) composites by Joule heating. In this study, we investigated the effectiveness of grafting silver-nanoparticle-decorated graphene oxide (GO) onto carbon fibers to improve the electrothermal properties and Joule-heating-activated shape recovery of SMP composites. Self-assembled GO was grafted onto carbon fibers to enhance the bonding of the carbon fibers with the polymeric matrix via van der Waal's forces and covalent crosslinking, respectively. Silver nanoparticles were further self-assembled and deposited to decorate the GO assembly, which was used to decrease the thermal dissimilarity and facilitate heat transfer from the carbon fiber to the polymer matrix. The carbon fiber was incorporated with SMP to achieve the shape recovery induced by Joule heating. We found that the silver-nanoparticle-decorated GO helped us achieve a more uniform temperature distribution in the SMP composites compared to those without decoration. Furthermore, the shape-recovery behavior and temperature profile during the Joule heating of the SMP composites were characterized and compared. A unique synergistic effect of the carbon fibers and silver-nanoparticle-decorated GO was achieved to enhance the heat transfer and a higher speed of actuation. © 2014 Wiley Periodicals, Inc. *J. Appl. Polym. Sci.* 2015, 132, 41673.

KEYWORDS: graphene and fullerenes; nanotubes stimuli-sensitive polymers; structure–property relations

Received 25 May 2014; accepted 20 October 2014

DOI: 10.1002/app.41673

INTRODUCTION

A high interest in smart materials has remained for a couple of decades, and a significant amount of effort has been dedicated to the development of environmentally sensitive polymers.^{1–3} As an important type of environmentally sensitive polymer, shape-memory polymers (SMPs) are able to recover their original (or permanent) shape upon exposure to the right stimulus.^{4–9} The big family of thermally responsive SMPs includes polyurethane, poly(ethylene oxide), polystyrene, and epoxy.^{4,10–12} These SMPs are generally deformed above the transition temperature and then cooled down to below the transition temperature to fix the deformed shape.^{13–16} This is a process known as *programming*. Recovery to the permanent shape is achievable only upon heating to above the transition temperature again, a process termed *recovery*.^{17,18} A combination of these process is a phenomenon called the *shape-memory effect* (SME).^{4,19–21} Unlike their metallic

counterpart, namely, shape-memory alloys, in which the reversible martensitic transformation between austenite and martensite is the underlying mechanism, the SME in SMPs is predominantly an entropic phenomenon.^{22–24} For any type of working mechanism, a structure of transition component and elastic is essential for SME in polymers.^{25,26} As one of the most popular environmentally sensitive materials, SMP has attracted great scientific and industrial interest because of its outstanding advantages, such as its light weight, high recoverable strain, ease in manufacturing, and properties that are tailorable to precisely meet the requirements of particular applications.^{27–30} However, there are some challenges that SMP must overcome before its full potential can be explored;^{25,31,32} these include a low recovery force, slow response speed, and poor thermal and electrical properties.³³ Research on the actuation approach for SMPs is in high demand to bridge the gap between scientific development and practical engineering applications. Recently, continuous efforts

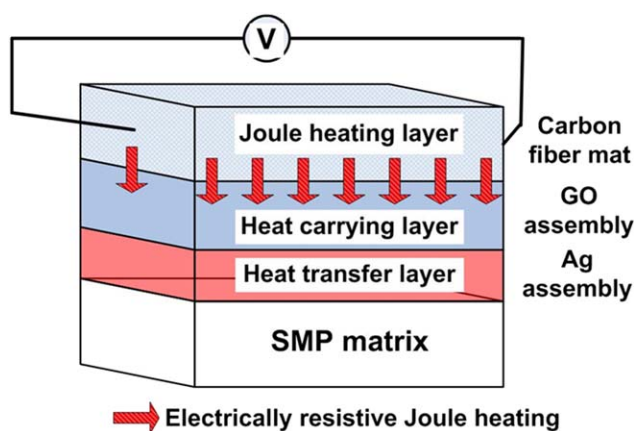


Figure 1. Schematic illustration of the synergistic effects of carbon-fiber and silver-nanoparticle-decorated GO on the electrical actuation of the SMP composite. [Color figure can be viewed in the online issue, which is available at wileyonlinelibrary.com.]

have been devoted to the modification of existing SMPs by means of loading with electrically conductive components, such as carbon nanofiber (CNF) mats,³³ carbon nanotubes,^{34,35} CNFs,^{36,37} carbon black,³⁸ short carbon fibers,³⁹ carbon nanotube alignment,⁴⁰ and nanopaper,^{41–43} to achieve electrically induced actuation.

Graphene oxide (GO) is able to improve the properties of polymers in many ways for new technological applications.^{44–46} Because of the potential covalent bonds, GO is able to function as a stand-alone structure, as a part of a structure, or in the reinforcement of polymers. A larger specific surface area provides a stronger connection between the carbon fibers and the polymer matrix. Even at a low volume fraction, the vast interfacial area created by well-dispersed GO can affect the behavior of the surrounding polymer matrix and create a cocontinuous network to fundamentally improve the physical properties of

the polymer composites.⁴⁷ In this study, we introduced a silver-nanoparticle-decorated GO assembly grafted onto carbon fibers to improve the electrothermal properties and electro-activated shape-recovery performance of SMP composites. The carbon fibers were incorporated into the SMP to achieve Joule-heating-induced shape recovery. GO self-assembled and was grafted onto the carbon fibers to enhance the interfacial bonding with the SMP matrix via van der Waal's forces and covalent cross-linking, respectively. Furthermore, the GO assembly was expected to act as a Joule-heat-carrying layer because of the excellent electrical and thermal conductivities in its basal plane. Silver nanoparticles were further used to decorate the GO assembly and work as a heat-transfer layer because of their exciting thermal conductivity. The silver-nanoparticle-decorated GO was used to decrease the thermal dissimilarity and facilitate heat transfer from the carbon fiber to the polymer matrix. A schematic illustration of the mechanism of the synergistic effect of the carbon fibers and silver-nanoparticle-decorated GO on the SMP composite is presented in Figure 1.

EXPERIMENTAL

The SMP matrix used in this study was an epoxy-based fully formable thermoset SMP resin, which was a two-part system of the resin matrix and curing agent. The glass-transition temperature (T_g) was 110°C. Cured epoxy-based SMP has a unique SME. When heated above or approximately to the T_g , it can change from a rigid plastic to an elastic rubber. Crystalline carbon-fiber plain-weave fabrics (T700) were purchased from Toray (Japan). The carbon fibers had a diameter of 7 μm and a volume resistivity of $1.5 \times 10^{-4} \Omega \text{ m}$ at 20°C. The CNFs were received in powder form and then heat-treated at 2200°C for 180 min to obtain complete graphitic structures and to allow them to purify themselves to a high level of greater than 99 wt %. The nanofibers had a diameter of 50–100 nm and a length of 30–100 μm .

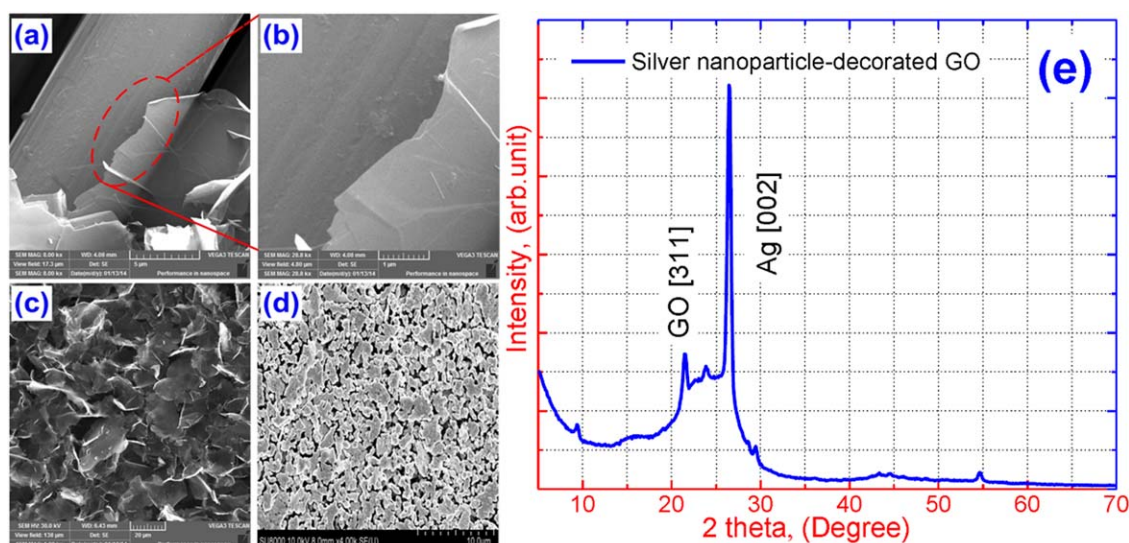


Figure 2. (a,b) Typical surface views of GO grafted onto carbon fibers at scales of 5 and 1 μm , respectively. (c) Morphology of the GO assembly. (d) Typical surface view of the silver nanoparticles. (e) XRD pattern of the silver-nanoparticle-decorated GO assembly in the range 5–70°. [Color figure can be viewed in the online issue, which is available at wileyonlinelibrary.com.]

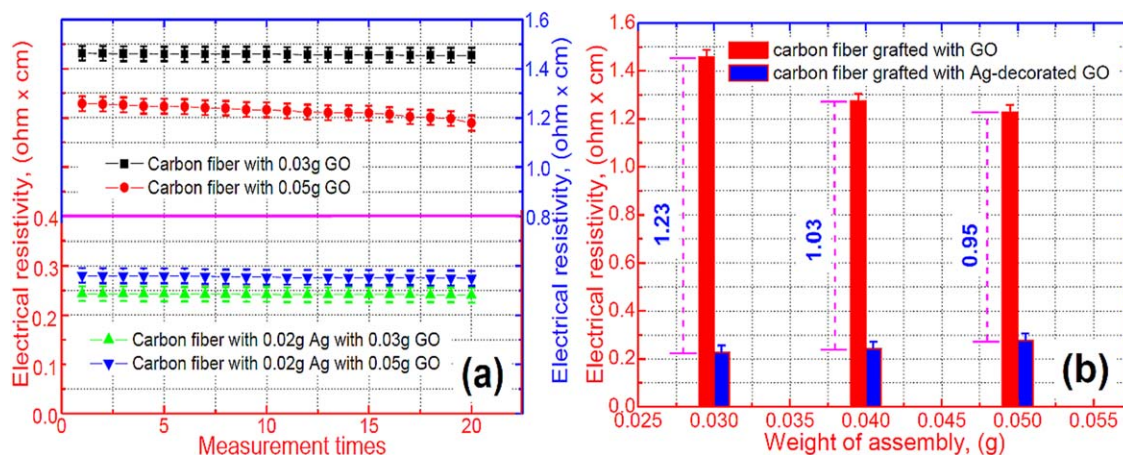


Figure 3. (a) Electrical resistivity of the carbon fiber mats grafted with the GO assembly and with the silver-nanoparticle-decorated GO assembly as a function of the measurement time. (b) Comparison of the electrical resistivity of the carbon fiber mats grafted with the GO assembly and with the silver-nanoparticle-decorated GO assembly. [Color figure can be viewed in the online issue, which is available at wileyonlinelibrary.com.]

GO was prepared and synthesized according to a modified Hummers' method. The raw graphite, NaNO_3 , and sulfuric acid were stirred together for 15 min below 5°C . A certain amount of KMnO_4 (>99.3%) was added step by step to the mixture, and stirring was maintained to keep the mixture temperature below 20°C . Then, the mixture was transferred into a 25°C water bath and stirred for 30 min to form a thick paste. Consequently, 200 mL of deionized water was added to the mixture, and this addition was accompanied by strong mechanical stirring. Subsequently, the mixture was further treated in 700 mL of deionized water and 60 mL of a 30% H_2O_2 solution. The resulting graphite oxide was dispersed in deionized water and sonicated for 1 h to obtain GO. The prepared GO (0.02, 0.03, 0.04, 0.05, and 0.06 g) was mixed with 60 mL of distilled water to form a suspension with the aid of the nonionic surfactant Triton X-100 [$\text{C}_{14}\text{H}_{22}\text{O}(\text{C}_2\text{H}_4\text{O})_n$]; this had a hydrophilic poly(ethylene oxide) group and a hydrocarbon lipophilic group. The GO suspension was then sonicated for 30 min. After that, the suspension was filtered under a high positive pressure to enable the GO to self-assemble and grafted onto carbon fibers through a hydrophilic polycarbonate filter membrane. After filtration, the GO assembly was dried in an oven at 120°C for 120

min to further remove the remaining water. Silver nanoparticles were then surface-coated on the GO assembly substrate to form a multifunctional laminate structure. Physical sputtering was used for the surface coating of the silver nanoparticles onto the GO assembly. It was driven by momentum exchange between the ions and atoms in the materials because of collisions. The primary silver particles for the sputtering process were supplied by an ion source. When such ions at a certain speed reach the target surface with an energy greater than the surface binding energy, an atom would be ejected; this is known as *sputtering*. Then, the atoms ejected collides with the substrate and coating. An amount of 0.02 g of silver nanoparticles was used to decorate the GO assembly. The carbon fiber mats grafted with silver-nanoparticle-decorated GO assembly were further heat-treated at 200°C for 30 min.

In the fabrication of the SMP composites, six pieces of carbon fiber mat grafted with silver-nanoparticle-decorated GO (with five different weight ratios of carbon fiber to silver nanoparticles to GO, namely, 0.14:0.02:0.02, 0.14:0.02:0.03, 0.14:0.02:0.04, 0.14:0.02:0.05, and 0.14:0.02:0.06) were placed at the bottom of a metallic mold. The SMP composites were fabricated by the

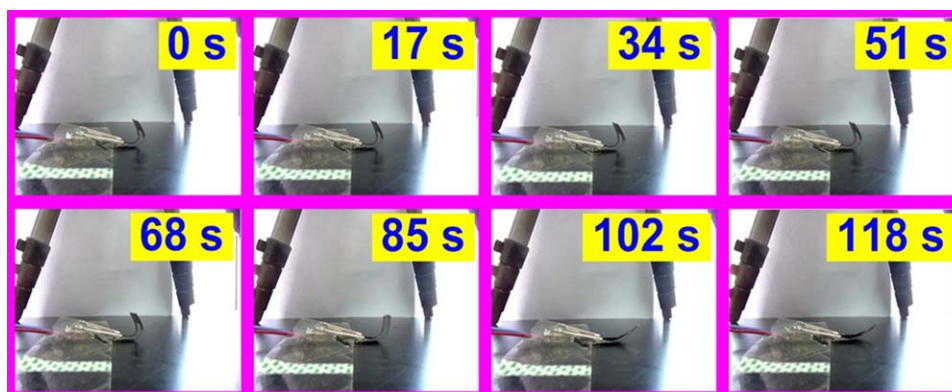


Figure 4. Snapshot of Joule-heating-induced SME of SMP composites incorporated with the carbon fiber mat grafted with the silver-nanoparticle-decorated GO assembly. [Color figure can be viewed in the online issue, which is available at wileyonlinelibrary.com.]

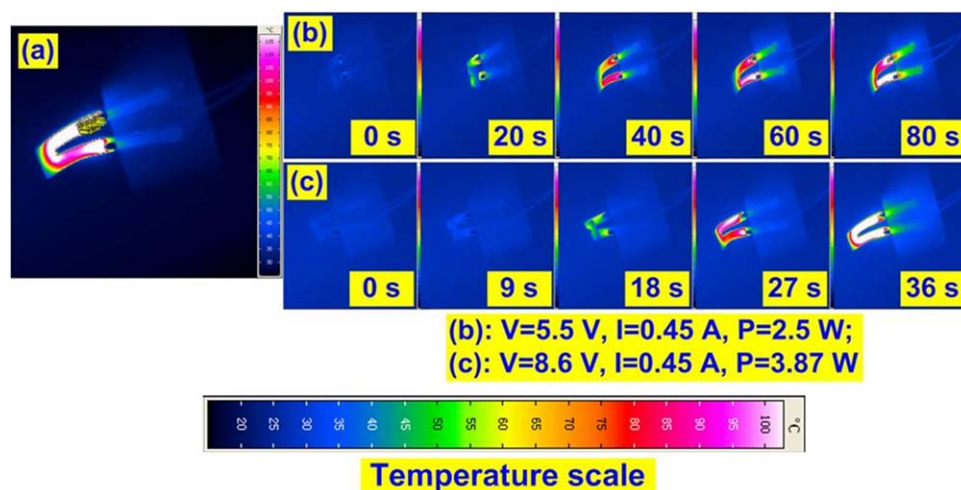


Figure 5. Snapshot of the Joule-heating-induced SME in the SMP composite. (a) Temperature scale. (b) Specimen enabled with the carbon fiber mat grafted with the GO assembly. (c) Sample enabled with the carbon fiber mat grafted with the silver-nanoparticle-decorated GO assembly. V: electric voltage; I: electric current; P: electric power. [Color figure can be viewed in the online issue, which is available at wileyonlinelibrary.com.]

coating of these carbon fiber mats onto the surface of SMPs via resin-transfer molding. The curing cycle is as follows: the cycle was ramped to 100°C at a heating rate of $1^{\circ}\text{C}/\text{min}$ and held for 5 h, it was then ramped to 120°C and held for 3 h, and finally, it was ramped to 150°C at 30°C per 120 min to produce the final SMP composite.

RESULTS AND DISCUSSION

Morphology of Carbon Fibers Grafted with a GO Assembly and Silver Nanoparticles

Typical surface morphologies of carbon fibers grafted with GO are shown in Figure 2(a,b), in which GO can be seen on the surface of the carbon fibers with different angles because of the high specific surface area of GO. With an increase in the weight fraction of GO, GO sheets can homogeneously cover the entire surface of carbon fibers to form a new hierarchical structure, as shown in Figure 2(c). The morphology and structure of the GO assembly decorated with silver nanoparticles are presented in Figure 2(d). The white areas correspond to the silver nanoparticle aggregates, with diameters ranging from 100 to 500 nm; they were uniformly deposited onto the GO assembly. Silver nanoparticles give rise to a homogeneous layer of the grafted GO assembly. We confirmed that these silver nanoparticle aggregates formed a continuously conductive network. The X-ray diffraction (XRD) pattern of the silver-nanoparticle-decorated GO obtained by mulberry leaf extract is shown in Figure 2(e). We found that the silver nanoparticles were evidenced by the peaks at 2θ values of 26.42° and 21.68° corresponding to (002) and (311) Bragg reflections of silver and GO, respectively. The XRD results show that the silver nanoparticles formed by the reduction of silver ions by the mulberry leaf extract were crystalline in nature. The narrow diffraction peak indicated a layer-to-layer diffraction distance (d -spacing) of 0.85 nm for the GO assembly.

Electrical Resistivity Measurement

The electrical resistivity of the resulting composites was determined by the van der Pauw four-point probe approach, which

is based on the electrical impedance measuring technique and uses separate pairs of current-carrying and voltage-sensing electrodes. The electrical resistivity of the carbon fiber mats grafted with the GO assembly and the silver-nanoparticle-decorated GO assembly is compared in Figure 3(a). The experimental results reveal that the average electrical resistivity decreased from 1.46 to $0.48\ \Omega\ \text{cm}$, when 0.02 g of silver nanoparticles was used to decorate the GO assembly (which was made from 0.03 g of GO). On the other hand, the average electrical resistivity decreased from 1.23 to $0.55\ \Omega\ \text{cm}$ when 0.02 g of silver nanoparticles was used to decorate the GO assembly (which was made from 0.05 g of GO). Figure 3(b) is a comparison of the

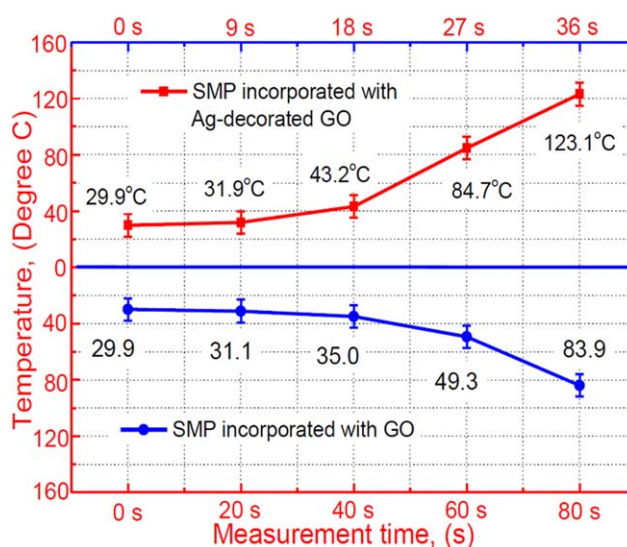


Figure 6. Highest temperature for the tested specimens: the SMP composite incorporated with the carbon fiber mat incorporated with the silver-nanoparticle-decorated GO assembly at 0, 9, 18, 27, and 36 s and the SMP composite incorporated with the carbon fiber mat incorporated with the GO assembly at 0, 20, 40, 60, and 80 s. [Color figure can be viewed in the online issue, which is available at wileyonlinelibrary.com.]

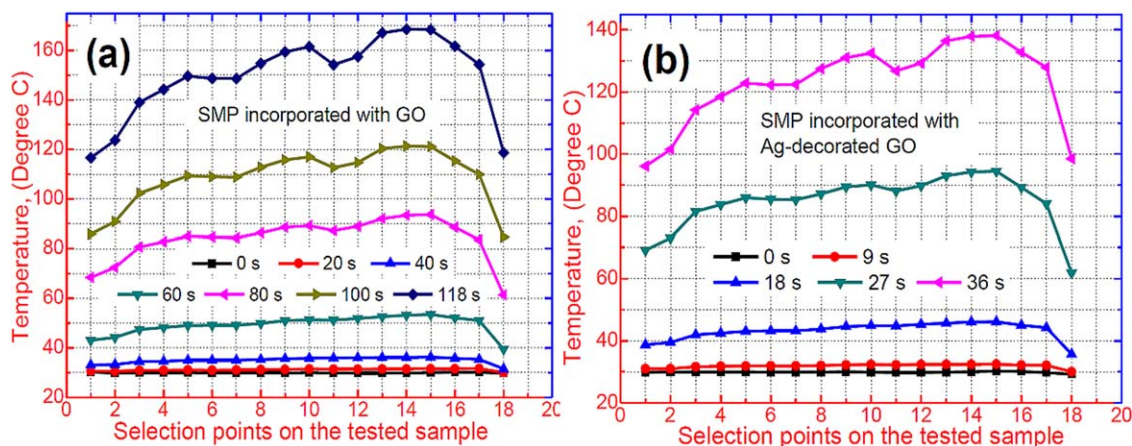


Figure 7. Temperature distribution curves of the SMP composites driven by Joule heating: (a) the SMP composite incorporated with the carbon fiber mat incorporated with the GO assembly and (b) the SMP composite incorporated with the carbon fiber mat incorporated with the silver-nanoparticle-decorated GO assembly. [Color figure can be viewed in the online issue, which is available at wileyonlinelibrary.com.]

electrical resistivity of the carbon fiber mat grafted with GO and that decorated with silver nanoparticles. We found that the electrical resistivity of the tested samples was significantly lowered after GO was decorated by the silver nanoparticles, and the electrical resistivity gradually decreased as the weight concentration of the GO assembly increased. We expected that with more GO loaded, the amplitude of the electric current and the current-carrying capability both decreased. The electrical conductivity along the thickness direction of the tested samples was measured to be smaller than that in its basal plane. On the other hand, the electrical resistivity gradually increased as the weight concentration of GO assembly increased in those decorated with silver nanoparticles. However, the electrical conductivity of the silver-nanoparticle-decorated GO seemed not to be as good as the carbon fibers; this resulted in an increase in the electrical resistivity with increasing amount of the silver-nanoparticle-decorated GO assembly. This may have contributed to the synergistic effect of the carbon fibers and the silver-nanoparticle-decorated GO assembly on the electrical resistivity of the tested specimens.

Electrically Induced Shape-Recovery Behavior

To demonstrate Joule-heating-induced shape recovery, two SMP composite samples (one SMP incorporated with carbon fiber mats grafted by GO assembly and the other incorporated with a carbon fiber mat grafted by the silver-nanoparticle-decorated GO assembly) were prepared with 0.14 g of carbon fibers and 0.03 g of GO. The originally flat sample with dimensions of $60 \times 4.5 \times 1 \text{ mm}^3$ was bent into an *n*-like shape (temporary shape) at 160°C and then cooled down to room temperature (22°C). No apparent shape recovery was found in the deformed sample in air for 60 min until an electric current of 0.45 A was applied for Joule heating. The shape-recovery behavior of the conductive SMP composites driven by an electric current was carried out and recorded by a video camera, as shown in Figure 4. The demonstrated specimen was cut out from the prepared SMP composite with dimensions of $120 \times 30 \times 2 \text{ mm}^3$. The specimen was then cut into a *n* shape to form a macro conductive path. The gap between the two legs of the specimen was 5 mm wide and

50 mm long. The specimen was bent into a *U* shape (temporary shape) at 150°C . This temporary shape was maintained until the specimen was cooled down to room temperature of 22°C . No apparent shape recovery was observed after the deformed specimen was kept in air for 30 min. An 8.6-V direct-current electric field was applied on the tested SMP composite for electrical actuation. In terms of electric power, approximately 3.87 W was applied during the electrical actuation experiment. With the electric power application, the tested SMP composite was heated to a high temperature by means of electrically resistive Joule heating. After the tested composite was heated to a temperature above its T_g , the stored mechanical energy in the composite was released. Here, the SMP macromolecules were activated, and SME was triggered. The SMP composite recovered its original shape from the deformed shape with the aid of electrically resistive Joule heating. The electrically induced shape-recovery process was slow within the initial 9 s. After about 10 s, the deployment speed of the SMP composite specimen dramatically increased. Electrically induced shape recovery was completed after 36 s of heating. The shape-recovery ratio of the SMP composite was approximately 98% compared with its original shape. The remaining deformation in shape might have resulted from the interfacial friction between the SMP matrix and silver-nanoparticle-decorated GO assembly. Furthermore, it must also be noted that the rate of shape recovery was strongly dependent on the magnitude of the applied voltage and the electrical properties of SMP composites. An IR video camera was used to simultaneously monitor the sequence of shape recovery and temperature distribution. A snapshot of both samples is revealed in Figure 5. Figure 5(a) presents the tested temperature location on the tested SMP composite specimen. The highest temperature of each sample was plotted, and the values are compared in Figure 6. We found that the sample with the GO assembly completed shape recovery in 118 s with an electric power of 2.5 W, as shown in Figure 5(b), whereas the sample with the silver-nanoparticle-decorated GO assembly took 36 s at an electric power of 3.87 W, as shown in Figure 5(c). Finally, the tested specimens showed a near 100% recovery ratio. Simultaneously, the temperature distribution on the silver-nanoparticle-decorated

SMP composite was more uniform than that of the GO-enabled sample. This contributed to the excellent thermal conductivity of the silver nanoparticles, which helped to facilitate heat transfer and resulted in faster shape recovery.

The temperature distribution along a specific line in both tested samples (at 18 selected points) is plotted in Figure 7. The high-temperature area was located in the deformed parts of the samples where the prestrain was higher than elsewhere. When electricity was applied, Joule heating resulted in a gradual temperature increase. The experimental results revealed that the SMP composite incorporated with a carbon fiber mat grafted with a silver-nanoparticle-decorated GO assembly reached the highest temperature of 123.1°C at 36 s; the temperature of the specimen incorporated with the carbon fiber mat grafted with a nondecorated GO assembly reached the highest temperature of 35.0°C at 40 s. Because of the synergistic effect of the carbon fiber and silver-nanoparticle-decorated GO assembly on the electrical and thermal conductivities of the SMP composites, the heating efficiency was significantly improved, and this resulted in a higher speed of recovery. A more uniform temperature distribution was also identified.

CONCLUSIONS

In this article, we have presented an effective approach for significantly improving the electrothermal properties and electro-activated shape-recovery performance of epoxy-based SMP composites incorporated with carbon fibers and a silver-nanoparticle-decorated GO assembly. GOs were self-assembled and grafted to significantly improve the heat-transfer capability in interfacial bonding between the carbon fibers and SMP matrix via van der Waal's forces and covalent crosslinking, respectively. Silver nanoparticles were further self-assembled and deposited to decorate GO and, thus, to decrease the thermal dissimilarity and facilitate heat transfer from the carbon fibers to the polymer matrix. Finally, the shape-recovery behavior and temperature profile during the electrical actuation of the SMP composites were characterized and compared. We found that the silver-nanoparticle-decorated GO was more helpful for achieving a more uniform temperature distribution within SMPs than that were undecorated. A unique synergistic effect of the carbon fibers and silver-nanoparticle-decorated GO was used to facilitate heat transfer and achieve high-speed electrical actuation of the SMP composites.

ACKNOWLEDGMENTS

This work was supported by the National Natural Science Foundation of China (contract grant numbers 11422217 and 51103032), the Program for New Century Excellent Talents in University (contract grant number NCET-13-0172), and the Foundation for the Author of National Excellent Doctoral Dissertation of the People's Republic of China (contract grant number 201328).

REFERENCES

1. Xie, T. *Polymer* **2011**, *52*, 4985.
2. Lu, H. B.; Yao, Y. T.; Huang, W. M. *Pigments Resin Technol.* **2013**, *42*, 237.
3. Lu, H. B.; Huang, W. M.; Wu, X. L.; Ge, Y. C.; Zhang, F.; Zhao, Y.; Geng, J. *Smart Mater. Struct.* **2014**, *23*, 067002.
4. Kim, B. K.; Lee, S. Y.; Xu, M. *Polymer* **1996**, *37*, 5781.
5. Mather, P. T.; Luo, X. F.; Rousseau, I. A. *Annu. Rev. Mater. Res.* **2009**, *39*, 445.
6. Lantada, A. D.; Morgado, P. L.; Sanz, J.; L. M.; Garcia, J. M.; Munoz Guijosa, J. M.; Otero, J. E. *Smart Mater. Struct.* **2010**, *19*, 055022.
7. Wang, C. C.; Huang, W. M.; Ding, Z.; Zhao, Y.; Purnawali, H. *Compos. Sci. Technol.* **2012**, *72*, 1178.
8. Meng, H.; Mohamadian, H.; Stubblefield, M.; Jerro, D.; Ibekwe, S.; Pang, S. S.; Li, G. G. *Smart Mater. Struct.* **2013**, *22*, 093001.
9. Lu, H. B.; Huang, W. M.; Leng, J. S. *Smart Mater. Struct.* **2014**, *23*, 045038.
10. Lendlein, A.; Kelch, S. *Angew. Chem. Int. Ed.* **2002**, *41*, 2034.
11. Lendlein, A.; Langer, R. *Science* **2002**, *296*, 1673.
12. Gall, K.; Dunn, M. L.; Liu, Y. P.; Stefanic, G.; Balzar, D. *Appl. Phys. Lett.* **2004**, *85*, 290.
13. Nguyen, T. D.; Qi, H. J.; Castro, F.; Long, K. N. *J. Mech. Phys. Solids* **2008**, *56*, 2792.
14. Xie, T. *Nature* **2010**, *464*, 267.
15. Lu, H. B.; Leng, J. S.; Du, S. Y. *Soft Matter* **2013**, *9*, 3851.
16. Xiao, R.; Nguyen, T. D. *Soft Matter* **2013**, *9*, 9455.
17. Miaudet, P.; Derre, A.; Maugey, M.; Zakri, C.; Piccione, P. M.; Inoubli, R.; Poulin, P. *Science* **2007**, *318*, 1294.
18. Lu, H. B. *Soft Matter* **2013**, *9*, 11157.
19. Sun, L.; Huang, W. M.; Ding, Z.; Zhao, Y.; Wang, C. C.; Purnawali, H.; Tang, C. *Mater. Des.* **2012**, *33*, 577.
20. Heuwers, B.; Beckel, A.; Krieger, A.; Katzenberg, F.; Tiller, J. C. *Macromol. Chem. Phys.* **2013**, *214*, 912.
21. Fejos, M.; Romhany, G.; Karger Kocsis, J. J. *Reinforced Plast. Compd.* **2012**, *31*, 1532.
22. Lu, H. B. *J. Appl. Polym. Sci.* **2012**, *123*, 1137.
23. Lu, H. B. *J. Appl. Polym. Sci.* **2013**, *127*, 2896.
24. Lu, H. B.; Huang, W. M. *Smart Mater. Struct.* **2013**, *22*, 105021.
25. Liu, C.; Qin, H.; Mather, P. T. *J. Mater. Chem.* **2007**, *17*, 1543.
26. Hu, J. L.; Zhu, Y.; Huang, H. H.; Lu, J. *Prog. Polym. Sci.* **2012**, *37*, 1720.
27. Buckley, P. R.; McKinley, G. H.; Wilson, T. S.; Small, W.; Benett, W. J.; Bearinger, J. P.; McElfresh, M. W.; Maitland, D. J. *IEEE Trans. Biomed. Eng.* **2006**, *53*, 2075.
28. Rousseau, I. A. *Polym. Eng. Sci.* **2008**, *48*, 2075.
29. Pretsch, T.; Ecker, M.; Schildhauer, M.; Maskosa, M. *J. Mater. Chem.* **2012**, *22*, 7757.
30. Zhao, Y.; Huang, W. M.; Wang, C. C. *Nanosci. Nanotechnol. Lett.* **2012**, *4*, 862.
31. Lu, H. B.; Liu, Y. J.; Leng, J. S.; Du, S. Y. *Appl. Phys. Lett.* **2010**, *97*, 056101.
32. Lu, H. B.; Liang, F.; Gou, J. H.; Huang, W. M.; Leng, J. S. *J. Appl. Phys.* **2014**, *115*, 064907.

33. Luo, X. F.; Mather, P. T. *Soft Matter* **2010**, *6*, 2146.
34. Cho, J. W.; Kim, J. W.; Jung, Y. C.; Goo, N. S. *Macromol. Rapid Commun.* **2005**, *26*, 412.
35. Lu, H. B.; Bai, P. P.; Yin, W. L.; Liang, F.; Gou, J. H. *Nano-sci. Nanotechnol. Lett.* **2013**, *5*, 732.
36. Lu, H. B.; Gou, J. H.; Leng, J. S.; Du, S. Y. *Smart Mater. Struct.* **2011**, *20*, 035017.
37. Tang, Z.; Sun, D.; Yang, D.; Guo, B. C.; Zhang, L. Q.; Jia, D. M. *Compos. Sci. Technol.* **2013**, *75*, 15.
38. Le, H. H.; Osazuwa, O.; Kolesov, I.; Ilisch, S.; Radosch, H. J. *Polym. Eng. Sci.* **2011**, *51*, 500.
39. Lu, H. B.; Yu, K.; Sun, S. H.; Liu, Y. J.; Leng, J. S. *Polym. Int.* **2010**, *59*, 766.
40. Lu, H. B.; Gou, J. H.; Leng, J. S.; Du, S. Y. *Appl. Phys. Lett.* **2011**, *98*, 174105.
41. Lu, H. B.; Gou, J. H. *Polym. Adv. Technol.* **2012**, *23*, 1529.
42. Lu, H. B.; Liang, F.; Yao, Y. T.; Gou, J. H.; Hui, D. *Compos. B* **2014**, *59*, 191.
43. Lu, H. B.; Huang, W. M.; Leng, J. S. *Compos. B* **2014**, *62*, 1.
44. Xing, G. C.; Guo, H. C.; Zhang, X. H.; Sum, T. C.; Huan, C. H. A. *Opt. Express* **2010**, *18*, 4564.
45. Dreyer, D. R.; Ruoff, R. S.; Bielawski, C. W. *Angew. Chem. Int. Ed.* **2010**, *49*, 9336.
46. McAllister, M. J.; Li, J. L.; Adamson, D. H.; Schniepp, H. C.; Abdala, A. A.; Liu, J. *Chem. Mater.* **2007**, *19*, 4396.
47. Kim, H.; Macosko, C. W. *Polymer* **2009**, *50*, 3797.